A ubiquitous *Microcoleus* species causes benthic cyanotoxic blooms worldwide

Authors:
Pilar Junier[1*], Guillaume Cailleau[1], Mathilda Fatton[1], Pauline Udriet[1], Isha Hashmi[1], Danae Bregnard[1], Andrea Corona-Ramirez[1], Eva de Francesco[1], Thierry Kuhn[1], Naïma Mangia[1], Sami Zhioua[1], Daniel Hunkeler[2], Saskia Bindschedler[1], Simon Sieber[3*], Diego Gonzalez[1*].

Affiliations:
[1]Laboratory of Microbiology, University of Neuchâtel, Switzerland
[2] Centre for Hydrogeology and Geothermics, University of Neuchâtel, Switzerland
[3] Department of Chemistry, University of Zürich, Switzerland

*co-corresponding authors:
Pilar Junier, Rue Emile-Argand 11, CH-2000, Neuchatel; pilar.junier@unine.ch; +41 32 718 22 44;
Diego Gonzalez, Rue Emile-Argand 11, CH-2000, Neuchatel; diego.gonzalez@unine.ch.
Simon Sieber, Winterthurerstrasse 190, CH-8057, Zurich; simon.sieber@uzh.ch

Abstract

In the last ten years, blooms of benthic cyanobacteria producing derivatives of the potent neurotoxin anatoxin-a have been repeatedly reported in rivers of temperate regions all over the world. For three series of events, in New Zealand, the USA, and Canada, a cohesive cluster of *Microcoleus* strains was found to be responsible for the toxin synthesis. Here, we document a similar toxigenic event that occurred at the mouth of the river Areuse in the lake of Neuchâtel (Switzerland) and caused the death of several dogs. Using 16S RNA-based community analysis, we show that benthic communities in the river are dominated by Oscillatoriales and especially by the *Microcoleus* genus. We correlate the detection of one specific sequence variant with the presence of anatoxin-a derivatives and use metagenomics to assemble a complete circular genome of the strain of interest. The strain is distinct from the ones isolated in New Zealand, the USA, and Canada, but belongs to the same species (>94% average nucleotide identity); it shares significant genomic traits with them, in particular a relatively small genome and incomplete vitamin biosynthetic pathways. Overall, our results suggest that the major anatoxin-a-associated benthic proliferations worldwide can be traced back to a single ubiquitous *Microcoleus* species rather than to a diversity of cyanobacterial lineages. We recommend that this species be monitored internationally and studied in detail in order to help predict and mitigate similar cyanotoxic events.

Introduction

Cyanobacterial blooms pose a significant threat to aquatic ecosystems and human health. They can interfere with the survival of both plants and animals by sequestering nutrients and causing oxygen depletion. Many cyanobacteria also produce toxic metabolites, collectively called cyanotoxins, which are active against a wide range of potential competitors and predators, from bacteria to vertebrates [1–6]. Commonly reported cyanotoxins in aquatic environments include microcystins, cylindrospermopsin, anatoxin-a congeners, and saxitoxins [7]. Because of their potency and wide

target-range, these toxins can by themselves profoundly affect the functioning of ecosystems [8]. They also represent a direct danger for human health during recreational activities and could have far-reaching and long-term consequences since some of them have been shown to bioaccumulate along the trophic chain [9].

While a majority of reported blooms are caused by cyanobacteria proliferating in the water column, blooms of substrate-attached, i.e. benthic, species are increasingly documented [10, 11]. This rise in benthic blooms is likely linked to human activities and, possibly, to global warming, which makes their investigation a pressing task [12, 13]. Benthic blooms typically start with the thickening and widening of bacterial mats on the bed of rivers and lakes [13]. At some point, the mats, loaded with oxygen entrapped in the filaments, detach from the substrate and reach the surface of the water bodies. Benthic blooms are associated with many different toxins, but most commonly with anatoxin-a [10]. Anatoxin-a (ATX) and its congeners, homoanatoxin-a (HTX), dihydroanatoxin-a (dhATX), and dihydrohomoanatoxin-a (dhHTX), are potent agonists of the nicotinic acetylcholine receptors [14]. They interfere with the function of neuromuscular junctions and can cause respiratory arrest in dogs and other vertebrates. ATX-producing benthic blooms have been reported from all over the world and particularly well documented in New Zealand (Hutt river, but many others), in the USA (Russian and Eel rivers), and more recently in Canada (Wolastoq river) [10, 14–21].

In New Zealand, the USA, and Canada, ATX-producing benthic blooms are caused by strains belonging to the *Microcoleus* genus (Oscillatioriales, section III) [22]. Due to the uncertainties of cyanobacterial taxonomy, these strains were initially classified as *Tychonema, Oscillatoria,* or *Phormidium,* but are progressively being renamed *Microcoleus* since a taxonomic clarification proposed in 2013 [23]. Among the ATX congeners, dhATX is the most commonly found in *Microcoleus*-dominated benthic blooms in New Zealand and the USA, while ATX seems the most frequent in Canada [19–21, 24]. Blooms typically comprise more than one strain with the overall toxin concentration correlating with the relative proportion of toxigenic to nontoxigenic strains [16, 25, 26]. Proliferation positively correlates with dissolved inorganic nitrogen-concentrations and in some studies with temperature and light intensity; lower phosphate concentrations also seem to favor blooms, possibly owing to the capacity of the implicated strains to efficiently mobilize phosphate from the substrate [13, 27, 28]. Like many closely-related Oscillatoriales, ATX-producing *Microcoleus* strains form long, intricated green to brown filaments, 5-10 µm in width; these filaments are composed of uniform cells with rounded or calyptra-covered cells at the tip of the filament and occasional necridia along the filament [23].

Partial, fragmented genomes have been assembled for several ATX-producing strains isolated in New Zealand, the USA, and Canada [20–22]. All these strains encode a specific variant of the ATX-biosynthesis cluster first described in *Cylindrospermum stagnale.* It comprises a short *anaG* allele leading to an ATX as the synthesis intermediate, rather than HTX. In addition, the presence of *anaK*, which encodes for an oxidase, is responsible for the transformation of ATX into dhATX [29, 30]. This is consistent with the detection of dhATX as the major ATX congener in these strains in New Zealand and the USA; some of the Canadian strains have *anaK* controlled by a different promoter that may be less active. Strains from New Zealand, the USA, and Canada are closely related at the nucleotide level (ANI>=94%) and have common genomic features compared to other *Microcoleus* strains, in particular a smaller genome size and missing genes in common vitamin biosynthetic pathways [22].

Here, we document a case of ATX-producing benthic cyanobacterial bloom, which happened in summer 2020 at the mouth of the Areuse in the Lake of Neuchâtel (Switzerland). This event entailed the death of six dogs and was followed by similar events in several other rivers and lakes in

Switzerland. We use 16S rRNA gene sequencing and metagenomics to identify the strains responsible for the toxin production and to survey the diversity of benthic cyanobacterial species in the river. While ATX-associated blooms and death of dogs have been reported in many rivers and lakes in Europe, this is the first such event that is fully documented at the genomic level.

Results

A cyanotoxic event associated with the proliferation of a Microcoleus *strain*

By the end of July 2020, six dogs died after being in contact with cyanobacterial scum close to the mouth of the river Areuse at the shore of the Lake of Neuchâtel (Switzerland). The toxicological analyses performed on the dogs and the scum identified anatoxin-a (ATX), a widespread toxin from cyanobacterial origin, as the most likely cause of death. The scum was particularly dense at the mouth of the Areuse, most likely because it originated from the river bed and got amassed in the delta by the backflow of the lake. The scum was composed of floating mats of entangled filaments often enclosing gas bubbles which increased their buoyancy, an appearance typical of benthic cyanobacterial blooms [10, 13].

To single-out the microorganisms responsible for the dogs' poisoning, we sampled the floating mats accumulating at the mouth of the river right after the event (July 31st) and two weeks later (August 16th) (Figure 1AB). Under the light microscope, the mats were mostly composed of filamentous cyanobacteria, greenish to dark-brown in color. Their trichomes presented a smooth morphology common to many benthic Oscillatoriales (Figure 1CD). Single cells were about 5-10 µm in width and square in shape, with hardly any constriction between individual cells and without sign of differentiation (no akinetes or heterocysts); at the tip of the filament, cells could be rounded or conical, and often bore calyptra. We narrowed down the taxonomic identification by sequencing a partial 16S rRNA gene amplicon using cyanobacterial primers (STable 1). Consistent with the microscopy, the closest matches of the consensus sequence in 16S rRNA gene databases were Oscillatoriales belonging to the *Microcoleus* genus (sometimes under their basonymes *Phormidium*, *Tychonema,* or *Oscillatoria*). To determine the full bacterial composition of the scum, we used high-throughput 16S rRNA gene amplicon (V3-V4 region) sequencing on the initial samples taken after the incident (end of July; 7cyano2) and a sample taken on the same site two weeks after (mid-August; 7cyano1). Floating mats were largely dominated by one *Microcoleus* strain, whose amplicon sequence variant (ASV) represented more than 65% of the bacterial reads in both samples (Figure 1EFG). Flavobacteria and Proteobacteria (*Rhodobacter, Rhodoferax, Brevundimonas*) were the most abundant heterotrophs in these samples (Figure 1EF). Overall, our observations and analyses suggested that the cyanotoxic event in the lake Neuchâtel was caused by the proliferation of at least one *Microcoleus* strain capable of producing an anatoxin-a congener.

Geographic origin, distribution, and diversity of blooming strains

We next addressed the geographic origin and distribution of the blooming strains along the river Areuse. In early September, we took multiple samples of cyanobacterial mats or biological material growing on immerged rocks, wood or sediments, at three main locations: in the delta on the river bed (11 samples, both mats and sediments; STable 1), on the banks along the last 1 km of the river (23

samples, both mats and sediments; STable 1), and at a dam located five kilometers upstream of the mouth, close to the village of Noiraigue (7 samples, floating mats only; STable 1). Floating mats were only observed near the mouth of the river and in Noiraigue. At the mouth of the river, the bed was almost entirely covered in dark microbial mats that resembled the floating scums (SVideo 1); these appeared to accumulate mainly in the delta of the river and were mostly absent on the lake floor (SVideo 2). A distinct type of floating cyanobacterial mats, whose color was bright green, was also collected in the lower part of the Areuse (samples 34, X, Y1 and Y2). While samples collected near the delta appeared clearly dominated by *Microcoleus*-like cyanobacteria under the microscope, the rock surface samples on the river banks contained a diversity of photosynthetic organisms, including cyanobacteria, algae and diatoms.

To get a sense of the diversity and frequency of filamentous cyanobacteria and, especially, of *Microcoleus* strains in the different samples, we performed high-throughput 16S rRNA gene amplicon sequencing (V3-V4 region) on extracted DNA. Filamentous cyanobacteria were largely dominant in scums and floating mats, representing up to 85% of all bacterial reads (Figure 2AB); they were very well represented in most other samples (sediments) with at least 20% of identified reads (with the exception of samples 100 and 200 from the upper Areuse). Among cyanobacteria, two operational taxonomic units could reach very high frequencies in a subset of samples: *Microcoleus*, present in most samples, and *Potamolinea,* dominating the four samples containing bright green filaments (samples 34, X, Y1, Y2). At the ASV level, the *Microcoleus* genus included a significant diversity with at least 20 different ASVs present across samples. One of these ASVs, identified as *Microcoleus anatoxicus* Stancheva & Conklin [20], was dominant in the scum and floating mats sampled in the delta and in the upper Areuse (Noiraigue). *Microcoleus* / *Tychonema* ASVs were more diverse in other samples especially in the mid-river bed. Like in the initial sampling, the most frequent heterotrophs across samples belonged to the Proteobacteria and Sphingobacteria (Flavobacteria) phyla.

Overall, these results indicate that *Microcoleus* strains are abundant in benthic mats in both their floating (blooming) and their surface-attached forms. One ASV in particular is associated with blooms in the lower and the upper Areuse.

A single Microcoleus *ASV is associated with a genetic marker for anatoxin-a and higher anatoxin-a and dihydro-anatoxin-a concentrations*

In parallel to the community profiling, we used published primers targeting the *anaC* gene to test each sample for the presence of the ATX biosynthesis cluster [31]. While virtually all the samples from the delta of the Areuse were positive for the *anaC* marker, the same marker was only detected in a quarter of the samples along the lower part of the river and in floating mats in the upper part of the Areuse (STable 1). This suggests that while the ATX producing strain is sporadically present on the bed and banks of the Areuse all along the river, it only reaches densities high enough to be detected by PCR in the delta region where the river current meets the backflow of the lake.

The presence of ATX and dhATX was confirmed by analyzing the samples by Ultra-high-performance liquid chromatography (UHPLC) coupled with a high-resolution mass spectrometer (HR-MS) [32] or a triple quadrupole mass spectrometer (TQMS) [33]. The extract from scum dominated by *Microcoleus* contained 0.1 % and 5% of ATX and dhATX respectively (11 µg of anatoxin-a and 241 µg of

dihydroanatoxin-a in a 8.2 mg of extract). In contrast, the samples dominated by *Potamolinea* contained less than 0.04% of ATX and dhATX (9.5 µg of anatoxin-a in 35.7 mg of extract).

All samples that tested positive for *anaC* contained a significant proportion of one *Microcoleus* ASV. While there was a clear association between that ASV and the ATX genetic marker, genomic data were still needed to formally demonstrate that the identified strain was the one actually encoding the ATX biosynthesis cluster.

The anatoxin-a-producing Microcoleus *from the Areuse is closely related to* Microcoleus *anatoxicus strains identified in New Zealand, the USA* and *Canada*

To formally identify the ATX-producing *Microcoleus* strain, we used a long-read high-throughput sequencing technology (Pacific Biosciences SMRT) to sequence DNA extracted from four samples. Three samples (A and N from the lower Areuse and 600 from the upper Areuse) were selected because they presented a high relative abundance of the *Microcoleus* ASV of interest and were positive for the *anaC* marker; the fourth sample (X from the lower Areuse) was chosen because it was dominated by the other blooming strain, *Potamolinea*. For all four samples, we obtained a number of large contigs that were binned based on coverage and tetranucleotide identity, and classified based on global homology and full 16S rRNA gene sequences (SFigures 1-4, STable 2). We were able to assemble the full circular genome of a *Microcoleus* strain for sample A and N, as well as large contigs of a *Microcoleus* strain for sample 600 and large contigs of a *Potamolinea* strain for sample X.

The full *Microcoleus* genomes assembled from samples A and N (strain NeuA/N) were virtually identical (>99.99% average nucleotide identity [ANI]) (SFigure 5). They significantly differed from the fragmentary genome assembled from sample 600 (Neu600) based on ANI (<90%) (Figure 3A), compositional binning (SFigure 1), and full 16S rRNA gene sequence (26 nucleotide differences over the whole sequence, although the closest match for both is *Microcoleus anatoxicus* PTRS2). Phylogenetically, all three strains belonged to the *Microcoleus-Tychonema* branch of Oscillatoriales, but several strains from public databases branched between strain NeuA/N and Neu600. The A/N strain forms a monophyletic clade with the dhATX producing strains from the USA and New Zealand (Figure 3A, SFigure 5) and shows very high homology with strains from the USA, New Zealand, and Canada (ANI >94%, alignment length >75%; Figure 3B, SFigure 6); this suggests that the toxic strains identified in all three countries belong to the same species. As expected, the contigs assembled from sample X (*Potamolinea* sp.) belonged to another main branch of the cyanobacterial phylogenetic tree, clustering with Coleofasciculates close to Nostocales (SFigure 5).

The genome of *Microcoleus* sp. NeuA includes one circular chromosome of 6.5 MB and one large circular plasmid of 0.1 MB; it encodes 5'687 protein-coding genes, 72 tRNAs, and three rRNA operons (Figure 3C). At the protein level, the strain shares many features with the dhATX-producing strains from the USA and New Zealand. A number of broad features distinguishes them from closely related strains that do not encode the dhATX biosynthesis cluster, in particular the presence of a geosmin biosynthesis cluster, a set specific of CRISPR/Cas proteins, and a large cluster of genes of uncertain function including several polysaccharide biosynthesis or modification enzymes.

Microcoleus sp. NeuA encodes a full ATX biosynthesis cluster comprising 10 genes (Figure 4A). This cluster includes a short *anaG* allele and the additional *anaK* gene characteristic of organisms that synthesize dhATX as their main toxin congener [29]. The complement and order of the genes is similar to the one found in the dhATX-producing *Microcoleus* strains from New Zealand, the USA, and Canada with the exception of a variable region, between *anaB-G* and *anaK-I*, encoding hypothetical or uncharacterized proteins (Figure 4A). Overall, these results confirm that the dhATX-producing *Microcoleus* strains from New Zealand, the USA, Canada, and Switzerland (NeuA/N) have similar properties including in terms of toxin-synthesis capacity. By contrast, the contigs assembled from sample 600 did not include an ATX biosynthesis cluster, even fragmentary. A detailed examination of the flanking regions of the ATX biosynthesis cluster and their homologues in the non-toxic strains, including strain 600, clearly shows three different genomic states (Figure 4B): i) an ancestral state before the insertion of the ATX biosynthesis cluster, found in *Tychonema bourrellyi* FEM_GT703, *Tychonema* sp. BBK16, and our *Microcoleus* sp. Neu600; ii) a state where the full cluster is present at the same position, found in *Microcoleus* sp. CAWBG639, PTRS1 and NeuA/N; and iii) a third state found in *Microcoleus* sp. EPA2 (USA), where most of the cluster has been excised with a leftover of a hundred bases. The phylogenetic tree in Figure 4C shows the most likely history of the strain family, showing the acquisition of the ATX biosynthesis cluster at the beginning of the crown branch and its subsequent loss on the EPA2 branch.

Besides the ATX cluster, the genome of *Microcoleus* sp. NeuA/N encodes three additional biosynthesis clusters that present homology with those of geosmin, anachelin (a cyanobacterial siderophore), and scytocyclamide (STable 3). The dhATX-synthesizing *Microcoleus* strains from New Zealand and the USA have been reported to differ from non-producing *Microcoleus* strains by several genomic traits, in particular a smaller genome size (<7MB) and the presence of incomplete or alternative metabolic pathways [22]. The traits reported in these reference genomes hold true for the NeuA/N Swiss strain, but are not always exclusive to toxigenic strains in our dataset. Overall, we find that, compared to nontoxic strains, the dhATX producers tend to lack some genes in vitamin biosynthetic pathways, namely thiamine (*tenA* coding for thiaminase II), pyridoxal (*pdxH* coding for pyridoxamine 5'-phosphate oxidase), and cobalamine (*cbiG* coding for cobalt-precorrin 5A hydrolase), to have more genes involved in sugar metabolism (for instance, UDP-glucose epimerase *galE*) and polysaccharide modification (sugar-kinases and phosphatases), as well as lipid and lipopolysaccharide metabolism, and to have a different set of CRISPR-cas9 associated proteins (SFigure 7-9).

Bacterial communities associated to different mat-forming cyanobacteria are distinct

Literature suggests that anatoxin-a-producing *Microcoleus* strains harbor specific cyanosphere-associated bacteria [34]. To test whether our data supported this hypothesis, we did a principal component analysis at the species level on the mat datasets, excluding all cyanobacterial ASVs. Samples dominated by *Microcoleus* sp. TycA, *Microcoleus* sp. 600, and *Potamolinea* sp. clustered separately, with three species belonging to the Sphingobacteriales—*Pedobacter* sp., *Paludibacter* sp., and *Flavobacterium* sp.—being the major drivers of the separation (Figure 5A). Consistent with this, a correlation analysis indicates that *Microcoleus* is positively correlated with the *Pedobacter* genus and negatively correlated with the *Potamolinea* genus (Figure 5B). A co-occurrence network analysis based on the lower Areuse samples confirms the association between *Microcoleus* sp. TycA and *Pedobacter* as well as the negative relation between *Microcoleus* sp. TycA and *Potamolinea* (Figure 5C). Overall,

these results strongly suggest that the bacterial communities assembled around different mat-forming cyanobacteria present a different composition.

Discussion

The event of dog poisoning registered in 2020 in Neuchâtel adds to an increasing list of episodes in which livestock, domestic animals, and even humans have been affected by the consumption of cyanotoxin-containing scums [35, 36]. Benthic cyanobacterial proliferations in rivers tend to form during the summer when water flows are more stable [35]. This is precisely the environmental setup in which the formation of floating mats containing cyanotoxins were detected in the Areuse. The general developmental cycle for benthic cyanobacteria typically starts with substrate colonization by filaments or hormogonia followed by mat formation. Flow, nutrients, and temperature interact to determine the mat development and accrual [13]. Once habitat has been colonized, subsequent proliferations become more likely [10]. In the Areuse, populations of potentially toxigenic species were detected in a large geographical area, suggesting that the toxigenic strain is well established and able to overwinter, making likely the occurrence of future blooms.

Although the presence of ATX-producing cyanobacteria was detected by PCR at multiple sites along the Areuse, floating and submerged mats, which most likely resulted from the clonal expansion of a single toxigenic *Microcoleus* strains (Figure 2D: ASV level), contained relatively high concentration of dhATX and ATX. By contrast, sediments and mats dominated by *Potamolinea* (e.g. Y, and X) contained low toxin concentrations (between 0.01 to 0.02% of the extract) (STable 1, Figure 2B). This is consistent with previous publications, which show that proliferation and scum formation can increase toxin levels by several orders of magnitude [37]. In the case reported here, the compound that actually led to the death of the dogs was most likely dhATX, whose concentration was about ten times higher than ATX in the mats (STable 1). Given the LD50 of dhATX (2.5 mg/kg by gavage), reported to be lower than ATX (10.6 mg/kg), the dogs would have had to ingest several grams of wet mats to reach the lethal dose [38].

The selective advantage ATX production might provide to producing strains is not clear and is likely unrelated with its effects on vertebrates. Studies on cultures of *Microcoleus autumnalis* revealed that ATX production was highest during early exponential phase, suggesting that ATX congeners may provide a physiological benefit during initial substrate colonization or when the producer's quorum is low in a mixed population [27, 39]. In such a context, ATX congeners could help control microherbivores like nematodes or crustaceans, for which ATX seems indeed to be toxic [40–42]. The toxins could also interfere with the metabolism of other cyanobacteria or algae and be effective as anti-competitor weapons [42, 43].

Two toxins, dhATX and ATX, as well as a genetic marker of the ATX biosynthesis cluster, were mainly detected in samples dominated by a single amplicon sequence variant belonging to a *Microcoleus* strain. This is consistent with recent literature on toxin benthic blooms, which repeatedly identified *Microcoleus* strains, sometimes referred to as *Tychonema* sp. or *Phormidium* sp., as major ATX congener producers in rivers [17, 21, 22, 44–46]. This ASV was present in a majority of submerged samples and was clearly dominant in floating mats (delta, river banks and upper Areuse) except in the bright green blooms dominated by *Potamolinea* (Figure 1D) [47]. This ASV (V3-V4 region) corresponds to the 16S rRNA gene sequence found in both *Microcoleus* sp. NeuA/N (dhATX producer) and *Microcoleus* sp. Neu600 (nonproducer), making them indistinguishable in the 16S rRNA gene community analysis. This highlights the co-occurrence of different closely related filamentous

cyanobacterial strains within benthic mats, which suggests that competition for dominance might actually be frequent in benthic communities. Sample 600 from the upper Areuse is an interesting case: it was dominated by the nonproducer strain Neu600 (based on the long-read shotgun sequencing data), but tested positive for *anaC* and presented levels of toxin similar to samples dominated by strain NeuA/N. This suggests that a small proportion of an ATX producing strain, maybe a close relative of NeuA/N, was present in the sample and possibly overproduced the toxins. Such cases of mixed blooms of ATX-producers and nonproducers have been commonly observed in New Zealand [26]. Whether interactions within such mats are cooperative—the toxic strain helping the nontoxic strain to proliferate, for instance by deterring crustaceans or worms—or competitive—the toxic strain slowly outcompeting the nontoxic one—is unknown. The presence of *Potamolinea* spp. also appears to limit the dominance of *Microcoleus* sp. and correlates with a lack of toxin detection. This may hint at potential competition between strains of the two genera. Future studies on the co-existence and/or competition between toxigenic and non-toxigenic *Microcoleus* species or between *Potamolinea* species and *Microcoleus* species may shed light on the population dynamics of benthic cyanobacteria.

Using high-throughput long-read sequencing of environmental samples, we successfully assembled a full circular genome for *Microcoleus* sp. NeuA/N (Figure 3). The genome encodes a variant of the ATX biosynthesis cluster known to generate dhATX as the main toxin congener, which is consistent with the toxicological results [22, 29]. While the organization of the locus is very similar to the ones found in the *Microcoleus* CAWBG639 and PTRS1-3 strains from New Zealand and the USA, as well as in contigs assembled from the Wolastoq river in Canada, it is clearly distinct from the model cluster found in *Cylindrospermum stagnale* (Nostocales) (Figure 4) [22, 29]; it is also distinct from the clusters found in phylogenetically closer benthic Oscillatoriales like *Kamptonema* PCC 6506, which produces HTX as its main congener respectively [30]. This highlights the diversity of extant ATX biosynthesis clusters in Cyanobacteria and their potential to synthesize a variety of chemical derivatives of ATX, some of which might still be unidentified. Compared to other Oscillatoriales, the genome of *Microcoleus* sp. NeuA/N is rather small with 6.5 MB plus a 100 kb plasmid. The size difference is partly due to a smaller number of secondary metabolite biosynthetic clusters and to a trend towards gene loss in conserved vitamin biosynthetic pathways (SFigures 6-8). These distinctive traits may be specific to the phylogenetic branch in which the ATX biosynthesis cluster got introduced or may represent subsequent adaptations to toxin production or growth in blooms.

Microcoleus/*Phormidium*-associated bacterial communities are thought to be quite similar across countries at higher taxonomic levels [48]. In our dataset, however, the bacterial communities assembled around benthic cyanobacteria appear to be species-specific at lower taxonomic levels (genus and species) (Figure 5): closely related species like *Microcoleus* sp. TycA and *Microcoleus* sp. 600, for instance, harbor clearly distinct communities (Figure 5A). We find that Sphingobacteriales (especially *Pedobacter* in our case) may play a central role in the economy of communities surrounding *Microcoleus* anatoxicus. Future studies should address whether the potential vitamin auxotrophies of the ATXc-producing *Microcoleus* strains may be balanced in nature by an association with specific strains, especially Sphingobacteriales, that may provide the missing compounds.

In conclusion, this study shows a clear convergence between cyanotoxic events happening at remote sites on the planet. These events are caused by strains belonging to a same species, based on ANI (>=94%), *M. anatoxicus*, which encodes a biosynthesis operon that produces dhATX as main toxic congener. These strains are capable of uncontrolled proliferation during warm seasons, during which their scums are a threat to mammals, especially dogs. We recommend that such blooms be reported and that specific management procedures be developed.

CRediT

Pilar Junier:	Investigation (equal), Conceptualization (equal), Methodology (equal), Funding (lead), Writing (equal), Project administration (lead), Review and editing (equal).
Diego Gonzalez:	Investigation (equal), Conceptualization (equal), Data curation (equal), Methodology (equal), Formal analysis (equal), Software (equal), Visualization (equal), Writing (equal), Review and editing (equal).
Guillaume Cailleau:	Visualization (equal), Investigation (equal), Conceptualization (equal), Data curation (equal), Methodology (equal), Formal analysis (equal), Software (equal), Review and editing (equal).
Simon Sieber:	Investigation (equal), Conceptualization (equal), Methodology (equal), Formal analysis (equal), Writing (supporting), Review and editing (equal).
Daniel Hunkeler:	Investigation (supporting), Review and editing (supporting).
Saskia Bindschedler:	Investigation (supporting), Review and editing (supporting).
Mathilda Fatton:	Investigation (supporting), Data curation (supporting).
Danae Bregnard:	Investigation (supporting), Data curation (supporting).
Pauline Udriet:	Investigation (supporting).
Isha Hashmi:	Investigation (supporting).
Andrea Corona-Ramirez:	Investigation (supporting).
Eva de Francesco:	Investigation (supporting).
Thierry Kuhn:	Investigation (supporting).
Naïma Mangia:	Investigation (supporting).
Sami Zhioua:	Investigation (supporting).

Acknowledgments

We thank Daniel Borel and Nathan Villat for their help during the sampling campaign.

Material and methods

Sampling. The sampling sites corresponded to three areas: (1) the mouth of the Areuse river, just before it connects to Lake Neuchâtel; (2) River delta, and (3) by a dam on the river in Noiraigue. The two first samples were taken at the mouth on July 31st, 2020, right after the death of several dogs, and on August 16, 2020, as part of a first monitoring of the evolution of the proliferation. On September 8th, 2020, a sampling campaign took place to establish the extent of the zone where cyanobacterial mats developed in the river and in the lake. The first series of samples came from the river banks, mats or sediments on rocks and other emerged surfaces (23 samples; codes A to Y). In addition, samples from underwater mats and sediments from the river mouth and from the delta were obtained by diving (numerical codes below 100). Finally, on September 11, 2020, a second sampling took place near the town of Noiraigue and included three stations: directly in the town, near an abandoned dam and upstream of the current dam (7 samples; numerical codes 100 and above; Table S1). All samples were collected using a spatula to transfer cyanobacterial mats/biomass into tubes as free of contamination as possible.

DNA extraction. 500 mg of biomass were added to Lysing Matrix E tubes containing phosphate and MT buffer and vortexed. The tubes were then placed in a Tissue Lyser for 10 minutes at 50Hz, with intermittent cooling on ice. After centrifugation to remove debris, the supernatant was transferred to new tubes. For protein precipitation, Protein Precipitation Solution was added to the supernatant. The mixture was left to precipitate at 4°C for 10 minutes, followed by centrifugation. The Binding Matrix suspension was added to the supernatant. After incubation, the mixture was filtered through SPIN™ filters; multiple rounds of filtration were conducted if necessary. DNA was eluted from the matrix at 55°C in 100µl H2O. Storage was done at -20°C.

16S PCR for Cyanobacteria identification. A 40-cycle polymerase chain reaction (PCR) was performed using specific primers for cyanobacteria, Cya106f (5'-CGG ACG GGT GAG TAA CGC GTG A-3') and Cya781R(b) (5'-GAC TAC AGG GGT ATC TAA TCC CCT T-3') with the AllinTM Red Taq DNA Polymerase (highQu GmbH, Kraichtal, Germany). Annealing temperature was 58°C. The amplicon was sequenced using the Sanger method (Microsynth A.G., Switzerland). The amplified DNA was then purified by depositing the PCR products in a 96-well MultiScreen PCR plate (Millipore). A vacuum of 15 inHg was applied to the wells containing the PCR products until all the wells were dry (12-15 minutes). 30 µl of sterile ultrapure water was added to the wells, which were then allowed to stand for 1 min. The samples were resuspended in ultrapure water by back and forth pipetting and transferred to Eppendorfs with a volume of 0.5 ml. Purified PCR products were quantified again using the Qubit fluorometer before being sent to Fasteris for Sanger sequencing. Each PCR product was sequenced in both directions. After sequencing, each sample had a forward sequence and a reverse sequence. These sequences were then compared to a database available online (GenBank®) using the NCBI Basic Local Alignment Tool (BLAST) web interface [49].

16S community sequencing. The V3-V4 region (universal primers Bakt_341F 5'-CCT ACG GGN GGC WGC AG-3' and Bakt_805R 5'-GAC TAC HVG GGT ATC TAA TCC-3') [50] was amplified with a sample barcoding to allow multiplexing and adapter ligation to enable sequencing on the Illumina MiSeq platform (2 x 300 bp paired end reads). Demultiplexed and trimmed sequence reads provided by Fasteris were processed using *QIIME2* [51] with *dada2* [52] for the denoising step. Reads were truncated to 478 bases, the optimal length based of q-scores; a minimal overlap of at least 12 identical bases between pair-end reads was required to build a full sequence. The sequences were taxonomically classified using *QIIME2*'s *VSEARCH*-based consensus taxonomy classifier [53] with the

Silva database [54], release 138, for 16S rRNA genes. The Silva database was fine-tuned using the RESCRIPt QIIME2 plugin [55], provided by the QIIME2 Team. Once the ASVs were determined, all ASVs represented in the template-free control samples were excluded from the corresponding culture collection. The co-occurrence network analysis was performed using *SpiecEasi* [56].

Pacific Biosciences (Pacbio) SMRT shotgun metagenomics. 1µg DNA extracted from four environmental samples (A, N, 600, X) was used to prepare standard bacterial Pacbio sequencing libraries (insert size: 9000 bps), Libraries were purified using Ampure beads and bound using Sequel® II Binding Kit 2.2. The libraries were sequenced on a Sequel II instrument as part of a 6-sample multiplexed run. Read count per sample was between 166'000 and 345'000, base count between 600M and 1800M. High fidelity reads were generated using Pacbio CCS.

Genome assemblies. Genome assemblies were generated from high-fidelity reads only using *flye* (v. 2.9.2) with the --pacbio-hifi, --meta and --min-overlap 1000 options and three rounds of polishing; assemblies were further polished using *racon* (v. 1.5.0) with default parameters; *dnaA* (genome) and *parA* (plasmids) homologs were used to fix the start of circular genomes using *circlator* (v. 1.5.5). Contigs were assigned to taxonomical categories using *kraken2* (online version on the bv-brc.org website). Contigs larger than 20kbps were binned using *Rtsne* (pca=TRUE, perplexity=5, theta=0.1, check_duplicates = F) based on average observed over expected pentanucleotide frequency values calculated based on an in-house script. Coverage values were derived from *flye* assembly reports. Average Nucleotide identity was calculated using the *pyani* script (https://github.com/widdowquinn/pyani).

Gene prediction and annotation. Standard annotation was carried out through the NCBI Prokaryotic Genome Annotation Pipeline (PGAP). Protein classification and pathway analyses were done using both the Kyoto Encyclopedia of Genes and Genomes (KEGG) online service (*blastKOALA*) and the comparative systems analysis of the BV-BRC website. The genomes used for comparisons were the following: *Oscillatoria_nigro-viridis* PCC_7112 (GCA_000317475.1), *Tychonema* sp. BBK16 (GCA_021648855.1), *Tychonema bourrellyi* FEM_GT703 (GCA_002412335.2), *Microcoleus* sp. CAWBG58 (GCA_020883045.1), *Microcoleus* sp. PH2017_15_JOR_U_A (GCA_020738445.1), *Microcoleus* sp. EPA2 (GCA_020882975.1), *Microcoleus* sp. CAWBG639 (GCA_020883025.1). For American *Microcoleus* strains PTRS1-3 (SRR10997082-4) and Canadian *Microcoleus* sequences (W3-F: SRR21374384, W3-E: SRR21374385, W5: SRR21374391, W3-J: SRR21374397), contigs were assembled from traces using *metaspades* (v. 3.15.5) with standard options. Proteome comparisons were carried out using the Proteome comparison service of BV-BRC (*Microcoleus* sp. strain A or *Oscillatoria nigro-viridis* PCC 7112 as reference proteomes) and plotted on the reference genome using the *circlize* R library. The secondary metabolite biosynthesis clusters were predicted using the online *antiSMASH* service.

Phylogenetic trees. 356 complete cyanobacterial genomes (nucleotides, proteomes, and annotations) were downloaded from NCBI. Large protein-based phylogenetic trees were built using *fasttree* with -wag and -gamma options from a multiple alignment, made using *muscle* or *kalign* with default parameters, of 28 concatenated conserved proteins (essentially ribosomal proteins). Large 16S rRNA phylogenetic trees were built using *fasttree* with -gtr option from a multiple alignment made using *muscle* with default parameters. A phylogenetic tree based on 28 concatenated conserved proteins for strains close to *Microcoleus anatoxicus* was built using *iqtree2* with automated optimization of the transition matrix; alignment was made using *muscle*.

Data availability. Metagenome-assembled genome sequences were deposited on the NCBI repository (bioproject PRJNA943188). 16S rRNA data were deposited NCBI (bioproject XXXXX).

Plots and figures. Figures were made using *R* (v. 3.14). The following *R* libraries were used: *ggplot2, pheatmap, circlize, biostrings, igraph*.

Analysis of anatoxin-a and dihydroanatoxin-a. The sample collected in early August was analyzed by Ultra-high-performance liquid chromatography (UHPLC) coupled with a high-resolution mass spectrometer (HR-MS) [32]. The samples collected in September (STable 1) were analyzed using a UHPLC coupled with a triple quadrupole MS (TQMS) and with a selected reaction monitoring strategy for ATX as published previously [33]. Briefly, the cyanobacteria samples were centrifuged (30 min, 4000 g) and the supernatant was discarded. Water (30 mL) was added to the biomass, the mixture was vortexed and centrifuged (30 min, 4000 g), and the solution was decanted and discarded. An aqueous MeOH soln. (30 mL, 50%) was added to the biomass, the mixture was sonicated (3 x 3min), centrifuged (30 min, 4000 g), and the supernatant was collected and dried under a gentle flow of nitrogen. An aqueous MeOH soln. (50%) was added to the samples to afford a concentration of 1 mg/mL of extract and the samples were directly analyzed by UHPLC-ESI-MS in positive mode (Ultimate 3000 LC, Thermo Fisher Scientific, coupled to a TSQ Quantum Ultra, Thermo Fisher Scientific). The column used was the Kinetex Polar C18 (50 x 2.1 mm, 2.6 µm), the flow rate was set up to 0.4 ml/min, the column oven temperature was at 40°C, and the solvent system used was composed of A (H_2O with 0.1% HCO_2H) and B (MeCN with 0.1% HCO_2H). The column was pre-equilibrated with 0% B for 1min, the gradient increased to 60% B over 3.5 min and to 100% over 0.05 min, and was kept to 100% B for 1.24 min. The detection was achieved using the SRM mode as previously reported [33] and a fragmentation from 166.2 to 130 was selected. For the quantification of dihydroanatoxin-a, the calibration curve was based on the SIM of anatoxin-a at 166.2 *m/z* and the concentration of dihydroanatoxin-a in the sample was calculated using the SIM mode at 168.2 *m/z*. The quantification was done using a calibration curve obtained using analytical standard solutions prepared with the commercially available anatoxin fumarate (Bio-Techne).

References

1. Catherine Q, Susanna W, Isidora E-S, Mark H, Aurélie V, Jean-François H. A review of current knowledge on toxic benthic freshwater cyanobacteria – Ecology, toxin production and risk management. *Water Research* 2013; **47**: 5464–5479.
2. Janssen EM-L. Cyanobacterial peptides beyond microcystins – A review on co-occurrence, toxicity, and challenges for risk assessment. *Water Research* 2019; **151**: 488–499.
3. Mehinto AC, Smith J, Wenger E, Stanton B, Linville R, Brooks BW, et al. Synthesis of ecotoxicological studies on cyanotoxins in freshwater habitats – Evaluating the basis for developing thresholds protective of aquatic life in the United States. *Science of The Total Environment* 2021; **795**: 148864.
4. Paerl HW, Otten TG. Harmful Cyanobacterial Blooms: Causes, Consequences, and Controls. *Microb Ecol* 2013; **65**: 995–1010.
5. Carpine R, Sieber S. Antibacterial and antiviral metabolites from cyanobacteria: Their application and their impact on human health. 2021.
6. Sieber S, Grendelmeier SM, Harris LA, Mitchell DA, Gademann K. Microviridin 1777: A Toxic Chymotrypsin Inhibitor Discovered by a Metabologenomic Approach. *J Nat Prod* 2020; **83**: 438–446.
7. Svirčev Z, Lalić D, Bojadžija Savić G, Tokodi N, Drobac Backović D, Chen L, et al. Global geographical and historical overview of cyanotoxin distribution and cyanobacterial poisonings. *Arch Toxicol* 2019; **93**: 2429–2481.
8. Zanchett G, Oliveira-Filho E. Cyanobacteria and Cyanotoxins: From Impacts on Aquatic Ecosystems and Human Health to Anticarcinogenic Effects. *Toxins* 2013; **5**: 1896–1917.
9. Ferrão-Filho A da S, Kozlowsky-Suzuki B. Cyanotoxins: Bioaccumulation and Effects on Aquatic Animals. *Marine Drugs* 2011; **9**: 2729–2772.
10. Wood SA, Kelly LT, Bouma-Gregson K, Humbert J, Laughinghouse HD, Lazorchak J, et al. Toxic benthic freshwater cyanobacterial proliferations: Challenges and solutions for enhancing knowledge and improving monitoring and mitigation. *Freshw Biol* 2020; **65**: 1824–1842.
11. Quiblier C, Wood S, Echenique I, Heath M, Aurelie V, Humbert J-F. A review of current knowledge on toxic benthic freshwater cyanobacteria - Ecology, toxin production and risk management. *Water research* 2013; **47**.
12. Puddick J, Kelly LT, Wood SA. Climate change and toxic freshwater cyanobacteria in Aotearoa New Zealand. 2022. Cawthron, New Zealand.
13. McAllister TG, Wood SA, Hawes I. The rise of toxic benthic Phormidium proliferations: A review of their taxonomy, distribution, toxin content and factors regulating prevalence and increased severity. *Harmful Algae* 2016; **55**: 282–294.
14. Colas S, Marie B, Lance E, Quiblier C, Tricoire-Leignel H, Mattei C. Anatoxin-a: Overview on a harmful cyanobacterial neurotoxin from the environmental scale to the molecular target. *Environmental Research* 2021; **193**: 110590.
15. Bouma-Gregson K, Kudela RM, Power ME. Widespread anatoxin-a detection in benthic cyanobacterial mats throughout a river network. *PLoS ONE* 2018; **13**: e0197669.
16. Heath M, Wood S, Ryan K. Spatial and temporal variability in Phormidium mats and associated anatoxin-a and homoanatoxin-a in two New Zealand rivers. *Aquat Microb Ecol* 2011; **64**: 69–79.
17. McAllister TG, Wood SA, Atalah J, Hawes I. Spatiotemporal dynamics of Phormidium cover and anatoxin concentrations in eight New Zealand rivers with contrasting nutrient and flow regimes. *Sci Total Environ* 2018; **612**: 71–80.

18. Thomson-Laing G, Puddick J, Laroche O, Fulton S, Steiner K, Heath MW, et al. Broad and Fine Scale Variability in Bacterial Diversity and Cyanotoxin Quotas in Benthic Cyanobacterial Mats. *Front Microbiol* 2020; **11**: 129.
19. Wood SA, Biessy L, Puddick J. Anatoxins are consistently released into the water of streams with Microcoleus autumnalis-dominated (cyanobacteria) proliferations. *Harmful Algae* 2018; **80**: 88–95.
20. Conklin KY, Stancheva R, Otten TG, Fadness R, Boyer GL, Read B, et al. Molecular and morphological characterization of a novel dihydroanatoxin-a producing Microcoleus species (cyanobacteria) from the Russian River, California, USA. *Harmful Algae* 2020; **93**: 101767.
21. Valadez-Cano C, Reyes-Prieto A, Beach DG, Rafuse C, McCarron P, Lawrence J. Genomic characterization of coexisting anatoxin-producing and non-toxigenic Microcoleus subspecies in benthic mats from the Wolastoq, New Brunswick, Canada. *Harmful Algae* 2023; **124**: 102405.
22. Tee HS, Wood SA, Bouma-Gregson K, Lear G, Handley KM. Genome Streamlining, Plasticity, and Metabolic Versatility Distinguish Co-occurring Toxic and Nontoxic Cyanobacterial Strains of *Microcoleus*. *mBio* 2021; **12**: e02235-21.
23. Strunecký O, Komárek J, Johansen J, Lukešová A, Elster J. Molecular and morphological criteria for revision of the genus *Microcoleus* (Oscillatoriales, Cyanobacteria). *J Phycol* 2013; **49**: 1167–1180.
24. Wood SA, Selwood AI, Rueckert A, Holland PT, Milne JR, Smith KF, et al. First report of homoanatoxin-a and associated dog neurotoxicosis in New Zealand. *Toxicon* 2007; **50**: 292–301.
25. Heath MW, Wood SA, Ryan KG. Polyphasic assessment of fresh-water benthic mat-forming cyanobacteria isolated from New Zealand: Benthic cyanobacteria in NZ. *FEMS Microbiology Ecology* 2010; no-no.
26. Wood S, Puddick J. The Abundance of Toxic Genotypes Is a Key Contributor to Anatoxin Variability in Phormidium-Dominated Benthic Mats. *Marine Drugs* 2017; **15**: 307.
27. Heath MW, Wood SA, Barbieri RF, RG Y, Ryan KG. Effects of nitrogen and phosphorus on anatoxin-a, homoanatoxin-a, dihydroanatoxin-a and dihydrohomoanatoxin-a production by Phormidium autumnale. *Toxicon* 2014; **92**: 179–185.
28. Wood SA, Atalah J, Wagenhoff A, Brown L, Doehring K, Young RG, et al. Effect of river flow, temperature, and water chemistry on proliferations of the benthic anatoxin-producing cyanobacterium *Phormidium*. *Freshwater Science* 2017; **36**: 63–76.
29. Méjean A, Dalle K, Paci G, Bouchonnet S, Mann S, Pichon V, et al. Dihydroanatoxin-a Is Biosynthesized from Proline in *Cylindrospermum stagnale* PCC 7417: Isotopic Incorporation Experiments and Mass Spectrometry Analysis. *J Nat Prod* 2016; **79**: 1775–1782.
30. Méjean A, Paci G, Gautier V, Ploux O. Biosynthesis of anatoxin-a and analogues (anatoxins) in cyanobacteria. *Toxicon* 2014; **91**: 15–22.
31. Kelly LT, Bouma-Gregson K, Puddick J, Fadness R, Ryan KG, Davis TW, et al. Multiple cyanotoxin congeners produced by sub-dominant cyanobacterial taxa in riverine cyanobacterial and algal mats. *PLoS One* 2019; **14**: e0220422.
32. Müller MJ, Dorst A, Paulus C, Khan I, Sieber S. Catch-enrich-release approach for amine-containing natural products. *Chem Commun* 2022; **58**: 12560–12563.
33. Turner AD, Turner FRI, White M, Hartnell D, Crompton CG, Bates N, et al. Confirmation Using Triple Quadrupole and High-Resolution Mass Spectrometry of a Fatal Canine Neurotoxicosis following Exposure to Anatoxins at an Inland Reservoir. *Toxins* 2022; **14**: 804.
34. Bouma-Gregson K, Olm MR, Probst AJ, Anantharaman K, Power ME, Banfield JF.

Impacts of microbial assemblage and environmental conditions on the distribution of anatoxin-a producing cyanobacteria within a river network. *ISME J* 2019; **13**: 1618–1634.
35. Wood SA, Kelly LT, Bouma-Gregson K. Toxic benthic freshwater cyanobacterial proliferations: Challenges and solutions for enhancing knowledge and improving monitoring and mitigation. *Freshwater Biology* 2020; **65**: 1824–1842.
36. Svircev Z, Lalic D, Bojadzija Savic G, Tokodi N, Drobac Backovic D, Chen L, et al. Global geographical and historical overview of cyanotoxin distribution and cyanobacterial poisonings. *Arch Toxicol* 2019; **93**: 2429–2481.
37. Ibelings BW, Backer LC, WE K, Chorus I. Current approaches to cyanotoxin risk assessment and risk management around the globe. *Harmful Algae* 2015; **49**: 63–74.
38. Puddick J, van Ginkel R, Page CD, Murray JS, Greenhough HE, Bowater J, et al. Acute toxicity of dihydroanatoxin-a from Microcoleus autumnalis in comparison to anatoxin-a. *Chemosphere* 2021; **263**: 127937.
39. Heath M, Wood SA, RG Y, Ryan KG. The role of nitrogen and phosphorus in regulating Phormidium sp. (cyanobacteria) growth and anatoxin production. *FEMS Microbiol Ecol* 2016; **92**.
40. Schwarzenberger A. Negative Effects of Cyanotoxins and Adaptative Responses of Daphnia. *Toxins* 2022; **14**: 770.
41. Haque F, Thimmanagari M, Chiang YW. Ultrasound assisted cyanotoxin extraction for nematode inhibition in soil. *Ultrasonics Sonochemistry* 2022; **89**: 106120.
42. Plata-Calzado C, Prieto AI, Cameán AM, Jos A. Toxic Effects Produced by Anatoxin-a under Laboratory Conditions: A Review. *Toxins* 2022; **14**: 861.
43. Chia M, Kramer B, Jankowiak J, Bittencourt-Oliveira M, Gobler C. The Individual and Combined Effects of the Cyanotoxins, Anatoxin-a and Microcystin-LR, on the Growth, Toxin Production, and Nitrogen Fixation of Prokaryotic and Eukaryotic Algae. *Toxins* 2019; **11**: 43.
44. Bauer F, Fastner J, Bartha-Dima B, Breuer W, Falkenau A, C M, et al. Mass Occurrence of Anatoxin-a- and Dihydroanatoxin-a-Producing Tychonema sp. *Mesotrophic Reservoir Mandichosee*. 2020. River Lech, Germany.
45. Fastner J, Beulker C, Geiser B. Fatal Neurotoxicosis in Dogs Associated with Tychoplanktic, Anatoxin-a Producing Tychonema sp. *Mesotrophic Lake Tegel*. 2018. Berlin.
46. Shams S, Capelli C, Cerasino L, Ballot A, Dietrich DR, Sivonen K, et al. Anatoxin-a producing Tychonema (Cyanobacteria) in European waterbodies. *Water Research* 2015; **69**: 68–79.
47. Martins MD, Branco LHZ. Potamolinea gen. nov. (Oscillatoriales, Cyanobacteria): a phylogenetically and ecologically coherent cyanobacterial genus. *International Journal of Systematic and Evolutionary Microbiology* 2016; **66**: 3632–3641.
48. Echenique-Subiabre I, Zancarini A, Heath MW, Wood SA, Quiblier C, Humbert J-F. Multiple processes acting from local to large geographical scales shape bacterial communities associated with Phormidium (cyanobacteria) biofilms in French and New Zealand rivers. *Sci Rep* 2018; **8**: 14416.
49. Johnson M, Zaretskaya I, Raytselis Y, Merezhuk Y, McGinnis S, Madden TL. NCBI BLAST: a better web interface. *Nucleic Acids Research* 2008; **36**: W5–W9.
50. Herlemann DP, Labrenz M, Jürgens K, Bertilsson S, Waniek JJ, Andersson AF. Transitions in bacterial communities along the 2000 km salinity gradient of the Baltic Sea. *ISME J* 2011; **5**: 1571–1579.
51. Bolyen E, Rideout JR, Dillon MR, Bokulich NA, Abnet CC, Al-Ghalith GA, et al. Reproducible, interactive, scalable and extensible microbiome data science using QIIME 2. *Nat Biotechnol* 2019; **37**: 852–857.
52. Callahan BJ, McMurdie PJ, Rosen MJ, Han AW, Johnson AJA, Holmes SP. DADA2:

High-resolution sample inference from Illumina amplicon data. *Nat Methods* 2016; **13**: 581–583.
53. Rognes T, Flouri T, Nichols B, Quince C, Mahé F. VSEARCH: a versatile open source tool for metagenomics. *PeerJ* 2016; **4**: e2584.
54. Quast C, Pruesse E, Yilmaz P, Gerken J, Schweer T, Yarza P, et al. The SILVA ribosomal RNA gene database project: improved data processing and web-based tools. *Nucleic Acids Research* 2012; **41**: D590–D596.
55. Robeson MS, O'Rourke DR, Kaehler BD, Ziemski M, Dillon MR, Foster JT, et al. RESCRIPt: Reproducible sequence taxonomy reference database management. *PLoS Comput Biol* 2021; **17**: e1009581.
56. Kurtz ZD, Müller CL, Miraldi ER, Littman DR, Blaser MJ, Bonneau RA. Sparse and Compositionally Robust Inference of Microbial Ecological Networks. *PLoS Comput Biol* 2015; **11**: e1004226.

A ubiquitous *Microcoleus* species
causes benthic cyanotoxic blooms worldwide

Authors:
Pilar Junier[1*], Guillaume Cailleau[1], Mathilda Fatton[1], Pauline Udriet[1], Isha Hashmi[1], Danae Bregnard[1], Andrea Corona-Ramirez[1], Eva de Francesco[1], Thierry Kuhn[1], Naïma Mangia[1], Sami Zhioua[1], Daniel Hunkeler[2], Saskia Bindschedler[1], Simon Sieber[3*], Diego Gonzalez[1*].

Figures

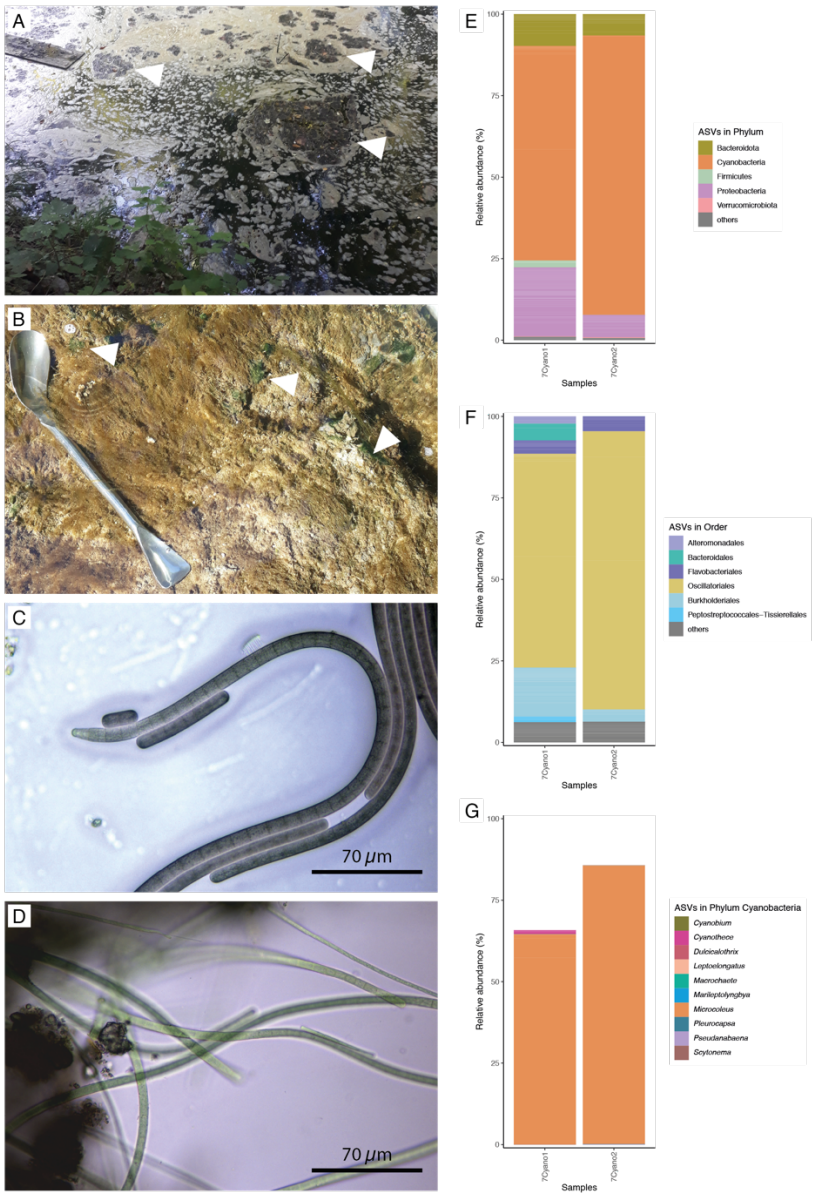

Figure 1. The initial toxigenic bloom event (July-August 2020). A. Mats and scum accumulating at the surface of the river close to the mouth of the Areuse. The low level of the river and a backflow of Lake Neuchatel created an area of low flow and accumulation of biomass in which scums (floating mats) were clearly observed. Arrows indicate floating mats among the scum. B. Benthic mats on stones with bright green patches (arrows) dominated by *Potamolinea* sp. C. Trichomes composing the toxigenic mats collected close to the mouth of the Areuse (dominant species. *Microcoleus* anatoxicus). These trichomes lack branching, heterocysts, and akinetes, and are characteristic of Oscillatoriales. Phase contrast microscopy, objective 100x. D. Trichomes composing the bright green mats collected close to the mouth of the Areuse (dominant species: *Potamolinea* sp.). Phase contrast microscopy, objective 100x. E. and F. The composition of the bacterial communities in the floating mats collected close to the mouth of the Areuse at Phylum (E) and the Order (F) levels. The communities present in two samples were analyzed on the basis of the V3V4 region of the 16S rRNA gene. G. The cyanobacterial fraction of the bacterial community is clearly dominated by *Microcoleus* at the genus level.

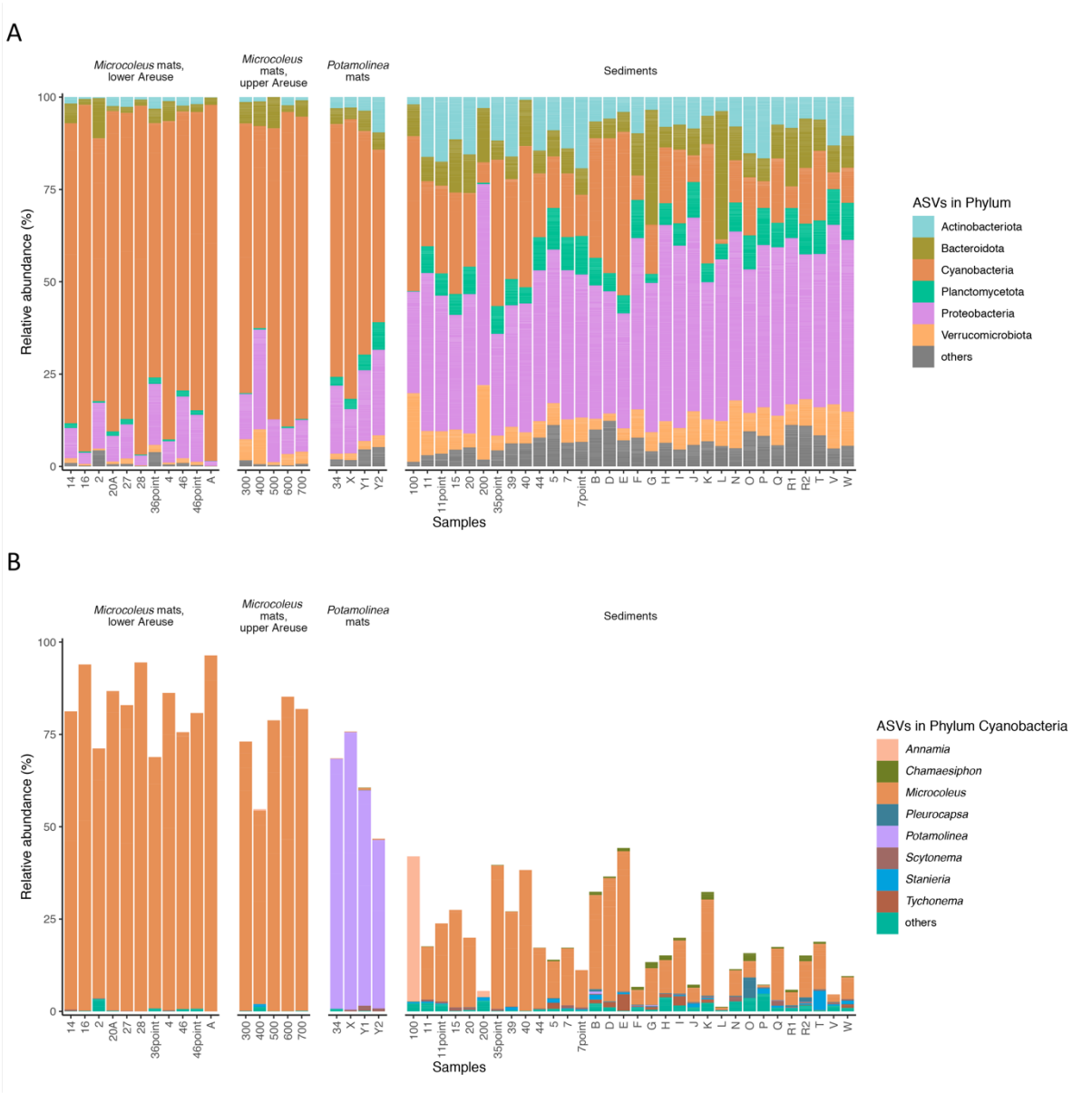

Figure 2. Composition of the bacterial communities present in mats and sediments from the Areuse in September 2020. The community composition is based on the V3V4 region of the 16S rRNA gene. The samples have been arranged by type (cyanobacterial mats *vs* sediments), dominant species (*Microcoleus vs Potamolinea*) and, for mats, by location (Lower Areuse *vs* Upper Areuse / Noiraigue). A. Community analysis at the phylum level, showing a substantial presence of Cyanobacteria and Proteobacteria in collected mats and sediments. B. Community analysis at the genus level, showing the dominance of *Microcoleus* in the cyanobacterial fraction of most samples.

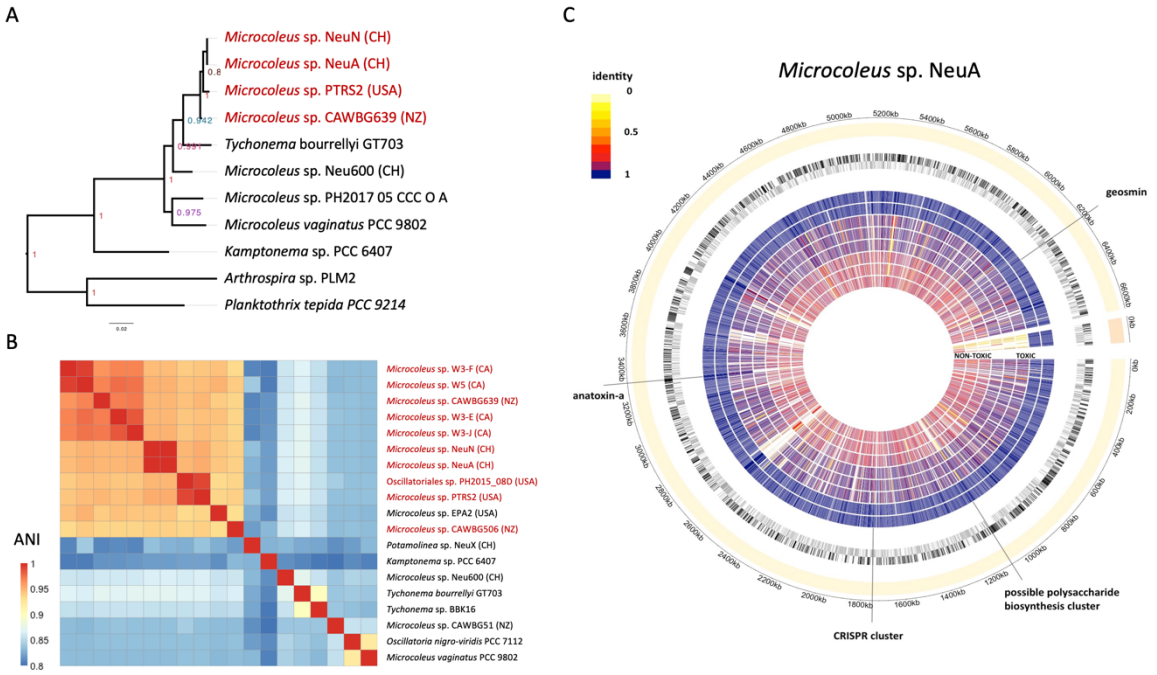

Figure 3. Phylogenomic characteristics of *Microcoleus* strains isolated from the Areuse. A. Phylogenetic tree of strains closely related to *Microcoleus* sp. NeuA based on 28 conserved proteins. The tree shows that dhATX-synthesizing strains from New-Zealand, the USA, and Switzerland belong to the same clade; *Microcoleus* sp. Neu600 branches before the acquisition of the dhATX biosynthesis cluster. B. Average nucleotide identity (ANI) among strains closely related to *Microcoleus* sp. NeuA. The figure indicates that NeuA/N (Switzerland), CAWBG639 (New Zealand), PTRS2 (USA), and four strains from the Wolastoq river (Canada) belong to the same species (ANI>=0.94). Both phylogeny and ANI suggest *Tychonema bourrellyi* GT703 and *Microcoleus* sp. Neu600 are the closest relatives of the dhATX-cluster encoding clade. C. Circular plot of *Microcoleus* sp. NeuA genome. From the exterior to the interior: a. molecules (yellow: genome; orange: plasmid) and coordinates; b. open reading frames (black: + strand; grey: - strand); c. protein identity value between reference (*Microcoleus* sp. NeuA) and *Microcoleus* sp. NeuA (toxic), NeuN (toxic), Neu600 (toxic), PTRS1 (toxic), CAWBG639 (toxic), EPA2 (lost dhATX cluster), Tyc600 (nontoxic), CAWBG58 (nontoxic), PH2017_15_JOR_U_A (nontoxic), PCC 7112 (nontoxic).

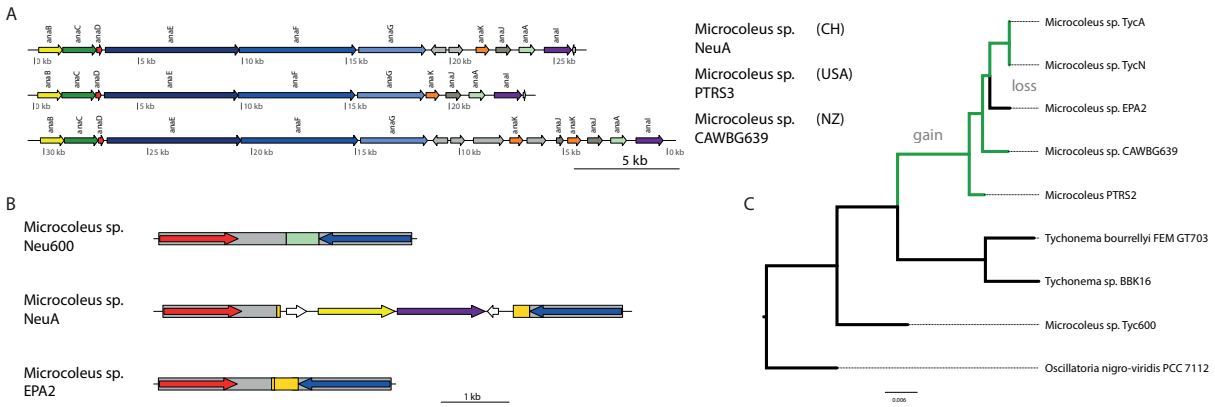

Figure 4. Sequence and evolution of the dhATX biosynthesis cluster in *Microcoleus* species. A. dhATX biosynthetic clusters from *Microcoleus* sp. NeuA, PTRS1 (USA), and CAWBG639 (NZ). The clusters are very conserved except for a variable region between the two parts of the cluster (*anaBCDEFG* and *anaKJAI*). B. The genomic context of the dhATX cluster in the ancestral nontoxic state (Neu600), after dhATX cluster acquisition (NeuA), and after secondary loss (EPA2). In green, a portion of DNA found in the ancestral state only; in orange, a portion of the dhATX biosynthesis cluster, which remains in EPA2 after cluster loss. C. Reconstruction of gain and loss events on a phylogenetic tree.

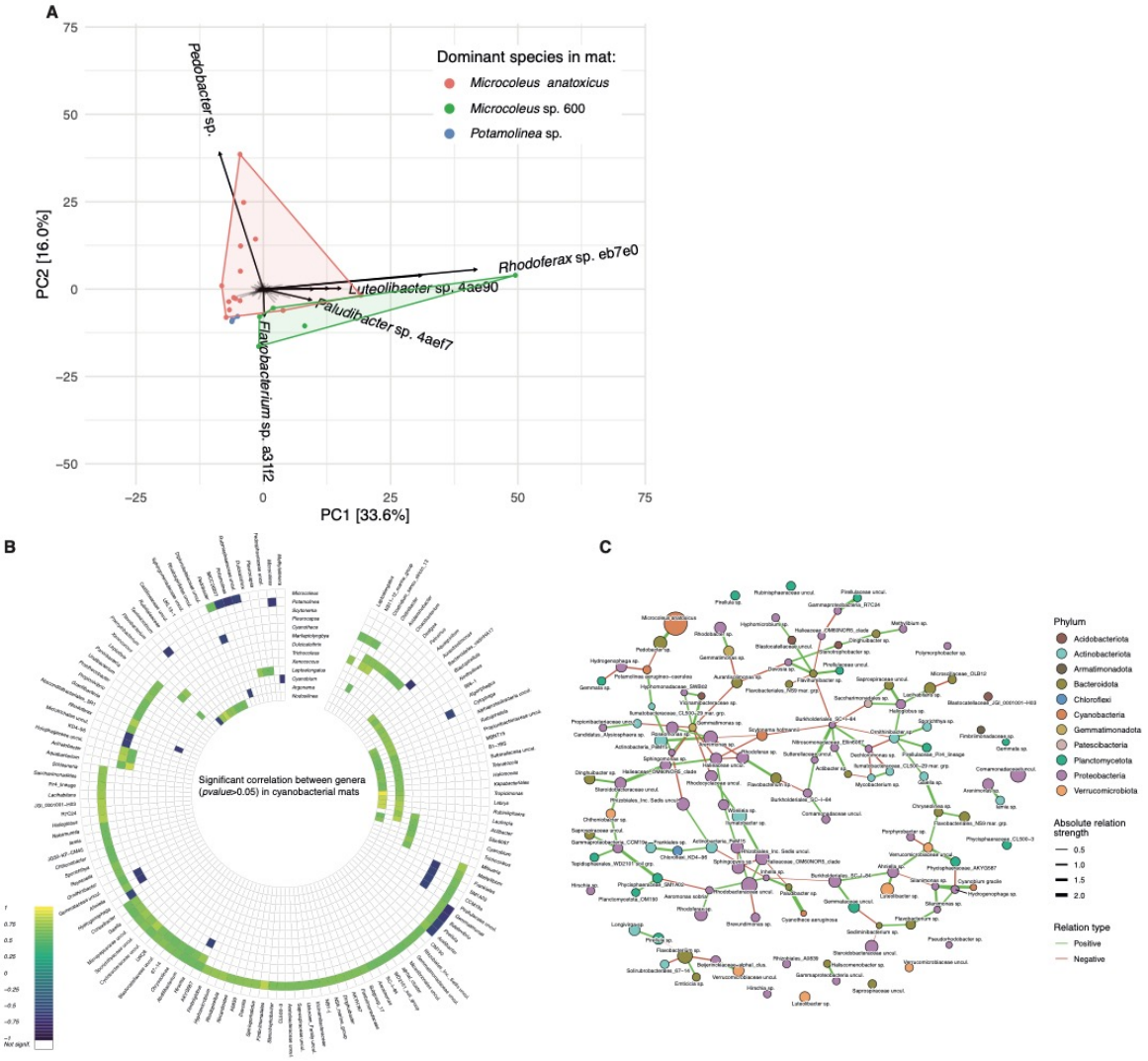

Figure 5. Bacterial communities in benthic mats differ in composition depending on the dominant cyanobacterial species. A. Principal component analysis (PCA) of bacterial communities in mat samples excluding all cyanobacterial ASVs (species level). All samples in the three first groups shown in Figure 2 are represented colored by the dominant cyanobacterium (*Microcoleus* sp. NeuA and sp. Neu600, *Potamolinea* sp.). The two first dimensions of the PCA are sufficient to separate the three groups of associated bacterial communities, which suggests that the communities are distinct from one another. B. Significant correlations (Spearman, p-value < 0.05) between cyanobacterial genera and all bacterial genera represented in more than two samples (mats only). C. Co-occurrence network reconstruction from the mat samples (excluding the upper Areuse mats), showing that the toxigenic *Microcoleus* species presents positive co-occurrence with *Pedobacter* sp. and negative co-occurrence with *Potamolinea* sp. Nodes are colored by Phylum; edge color indicates positive or negative co-occurrence; edge width represents co-occurrence strength.